ELSEVIER

Journal of Power Sources 91 (2000) 202–209

JOURNAL OF POWER SOURCES

www.elsevier.com/locate/jpowsour

Influence of flow field design on the performance of a direct methanol fuel cell

A.S. Aricò *, P. Cretì, V. Baglio, E. Modica, V. Antonucci

C.N.R.-T.A.E. Institute for Transformation and Storage of Energy, Salita S. Lucia sopra Contesse 39, 98126 S. Lucia, Messina, Italy

Received 25 January 2000; accepted 8 March 2000

Abstract

Serpentine (SFF) and interdigitated (IFF) flow fields were investigated with regard to their use in a direct methanol fuel cell (DMFC). The DMFC equipped with SFFs showed lower methanol cross-over, higher fuel utilisation and slightly larger voltage efficiency at low current densities. IFFs enhanced mass transport and membrane humidification allowing to achieve high power densities of 450 and 290 mW cm^{-2} in the presence of oxygen and air feed, respectively, at 130°C. A fuel efficiency of 90% was obtained with the IFFs in the presence of 1 M methanol feed at 130°C and a current load of 500 mA cm^{-2}.

Keywords: Direct methanol fuel cells (DMFCs); Pt–Ru catalysts; Interdigitated flow fields; Mass-transport; Unsupported catalysts; Fuel cell performance

1. Introduction

Solid polymer electrolyte direct methanol fuel cells (DMFCs) have achieved significant levels of performance in the last years [1–7]. Various technical approaches have contributed to the amelioration of the electrochemical characteristics. These mainly concern the choice of thin film, highly conductive, protonic membranes, which allow the operation of fuel cells at temperatures close or above 100°C and the development of highly active anodic catalysts [1,7]. In this regard, an increase of fuel cell temperature produces a corresponding enhancement of the methanol reaction kinetics, which compensates for the electrochemical losses due to increased methanol cross-over across the membrane. Among the various catalysts investigated for the methanol electro-oxidation [8–11], the Pt–Ru system shows significant advantages since the high intrinsic catalytic activity of such a bifunctional catalyst can be combined with a high active surface area [7]. Furthermore, unsupported or high metal concentration carbon-supported anode and cathode catalysts have been successfully used in DMFCs in recent years [1,7]. These materials allow the fabrication of catalytic layers with a small thickness, thus, favouring the diffusion of reactants to the catalytic sites [1].

The reduction of kinetic and ohmic limitations at high operation temperatures determines an increase of the influence of mass-transport limitations to the polarisation characteristics. In this regard, some progress has been obtained by improving the characteristics of the backing layer in terms of composition and thickness. Nowadays, a few investigations have been extended to the reactant flow fields [12–16]. Actually, the most widely employed flow field in small fuel cell devices is based on the so-called serpentine configuration. In such configuration, the reactant is constrained to flow along parallel channels, which are machined in a graphite plate in contact with the electrode backing layer. Such design is often adopted for stacked cells. The reactant molecules have access to the catalytic sites through diffusion across the so-called diffusion layer, i.e. the backing layer, made of carbon cloth and carbon black and hydrophobized by appropriate addition of polytetrafluoroethylene (PTFE).

Recently, a different approach for the flow of reactants and products inside the electrode structure, i.e. an interdigitated design, was proposed by Nguyen [12] and Wilson et al. [13] for H_2–O_2 solid polymer electrolyte fuel cells (SPEFCs). In practice, the reactant gases are forced to enter into the electrode pores and exit from them under a gradient pressure by making the inlet and outlet channels

* Corresponding author. Tel.: +39-090-624-234; fax: +39-090-624-247.

E-mail address: arico@itae.me.cnr.it (A.S. Aricò).

0378-7753/00/$ - see front matter
PII: S0378-7753(00)00471-7

dead-ended. As pointed out by Nguyen [12], the flow through the electrode, in the presence of the interdigitated design, is no more governed by diffusion but becomes convective in nature. This particular design was selected for H_2–air SPEFCs in order to avoid the water flooding problem at the cathode and to facilitate the removal of inert nitrogen molecules, which accumulate in the catalyst pores producing a diffusion barrier [12]. The forced-flow-through characteristics created by the interdigitated flow fields (IFFs) in SPEFCs have been further investigated by various authors [14–16]. In general, it has been shown that enhanced mass transfer characteristics are achieved with the IFF.

Beside mass transport, the flow fields in a DMFC device play also a significant role on the characteristics of membrane hydration and cathode poisoning. These aspects greatly influence system efficiency. At low temperatures, although current densities in a DMFC are significantly lower than in a SPE fuel cell, the problem of water flooding at the cathode is still present. Whereas, cell operation at high temperatures imposes an efficient water transport from the cathode to the membrane. This phenomenon is less demanding at the anode, since the supply of a mixture of methanol and water allows appropriate membrane humidification on this side.

In the methanol fuel cell, an effective mass-transport of oxygen molecules to the cathode active sites has a two-fold role: (i) supply of reacting molecules at a rate compatible with the reaction kinetics, (ii) uniform supply of oxidant over reaction sites in order to counteract the effects of the electrochemical oxidation of methanol molecules crossing the membrane. When a significant oxygen depletion occurs in the cathodic layer, methanol molecules that have reached the cathode compartment readily chemisorb on the electrode surface with subsequent oxidation to CO_2. This determines a "mixed potential", which decreases the cell potential. The negative effects produced by the oxidation of such methanol molecules become less significant, if a fast and homogeneous distribution of oxygen molecules is present over the cathode surface. Accordingly, when air is supplied to the cathode, the cell performance significantly diminishes as a consequence of lower oxidant partial pressure and increased cathode polarisation due to the larger catalyst poisoning by methanol cross-over.

In the present work, the electrochemical behaviour of a DMFC in the presence of serpentine flow fields (SFFs) and IFFs at both cathode and anode was investigated. The cell was operated at temperatures of 100°C and 130°C in order to evaluate the influence of both kinetic and mass-transport limitations. In-house made unsupported Pt–Ru and 90% Pt/Vulcan XC catalysts were employed at the anode and cathode compartments, respectively, in conjunction with Nafion 112 membrane. The crystallographic structure and particle size of the catalysts employed in the present study were investigated by X-ray diffraction.

2. Experimental

Unsupported Pt–Ru (1:1) and 90% Pt/Vulcan XC 72 catalysts were in-house synthesised by using a colloidal procedure based on a modification of the "Prototech method" developed by Petrow and Allen [17]. Sulphite complexes of Pt or Pt and Ru were decomposed by hydrogen peroxide at 80–90°C to form aqueous colloidal solutions of Pt and Ru oxides. The colloidal Pt particles were adsorbed on a carbon black to form the Pt/Vulcan XC 72 catalyst, whereas, colloidal Pt–Ru particles were precipitated from the solution at pH5. The resulting amorphous oxides were reduced in a hydrogen stream.

X-ray diffraction analysis was carried out with Philips X-pert diffractometer using a CuKα source. The electrodes were prepared according to a procedure described in a previous paper [7]. They consisted of carbon cloth, diffusion layer and catalytic layer. Nafion content in the catalytic layer was 15% wt. The Pt loading in each electrode was 2 mg cm^{-2}. Membrane-electrode assemblies were formed by a hot-pressing procedure [18] and subsequently installed in a fuel cell test fixture of 5-cm^2 active area. The cell fixture was equipped either with a conven-

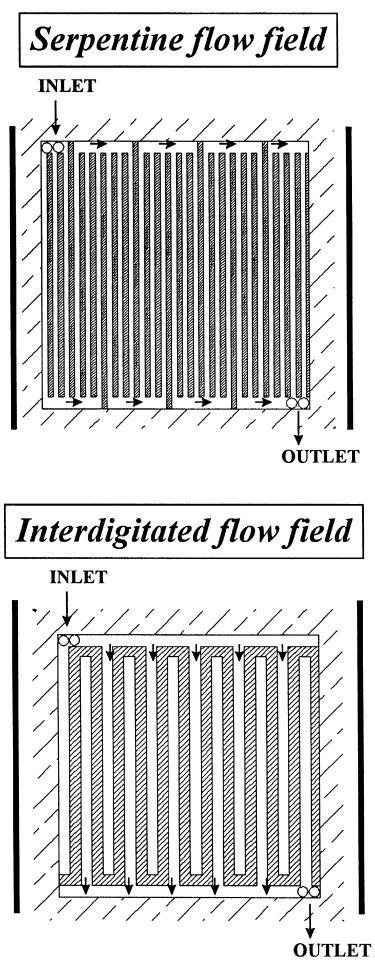

Fig. 1. Comparison of SFF and IFF designs.

tional serpentine graphite flow field (Globetech, College Station, TX) or with house-made interdigitated graphite flow fields based on a design similar to that reported by Nguyen [12]. The designs of graphite flow fields used in this work are reported in Fig. 1. The single cell test fixture was connected to a test station equipped with an HP6060B electronic load. Aqueous methanol was vaporised in a pre-heater kept at 140°C before being fed to the anode chamber of DMFC through a peristaltic pump; the temperature at the inlet of the cell was close to 100°C; humidified oxygen or air pre-heated at 100°C was circulated through the cathode chamber. Pressure in the anode compartment was varied depending on the operating temperature (1.5 atm at 100°C and 2.5 atm at 130°C), whereas, in the cathode compartment, it was fixed at 3 atm through back-pressure regulators. Reactant flow rates were 2 and 500 ml min^{-1} for the methanol/water mixture and air/oxygen stream, respectively. The fuel cell performance was investigated by steady-state galvanostatic measurements, while ohmic resistance was determined by the current-interrupter method using an oscilloscope.

The methanol cross-over was determined by the following procedure. Water and unreacted methanol in the outlet stream from the cathode were condensed in a reservoir; this solution was analysed by a Carlo Erba VEGA Series 2 GC 6000 chromatograph equipped with Carbopack 3% SP 1500 column and flame ionisation detector. Whereas, the gas composition containing air/oxygen and CO_2 was chromatographically analysed by drawing with a syringe a dried gas sample from a glass sampling bulb provided with a plug-type system. The gaseous products were analysed with a Hewlett-Packard 5890A gas-chromatograph equipped with two columns in series: (i) a 2.5-m Porapak QS 80/100 and (ii) a 2.5-m Molecular Sieve 5 A kept at 70°C connected to a thermal conductivity detector (TCD).

3. Results and discussion

3.1. X-ray diffraction analysis

X-ray diffraction was carried out on both unsupported Pt–Ru (1:1) and 90% Pt/C catalysts. Both catalysts exhibited the diffraction peaks of Pt or Pt–Ru fcc structure (Fig. 2). The (002) reflection of the graphitic basal plane of carbon black is not observed in the 90% Pt/C catalyst due to the high Pt concentration (Fig. 2). This peak should occur at about 25° (2θ). A significant shift to higher 2θ values is observed for the diffraction peaks in the Pt–Ru catalyst with respect to the Pt/C catalyst (Fig. 2). Such shift is due to the lattice contraction caused by Ru atoms. The lattice parameters, a_{fcc}, were 3.92 Å and 3.87 Å in the Pt/C and Pt–Ru catalysts, respectively. For a solid solution of Pt and Ru, there is a direct relationship between the lattice parameter, a_{fcc}, and the bulk composition [19]. Accordingly, the atomic fraction of Ru in the in house made Pt–Ru catalyst is 48 ± 2 %. In both catalysts, the mean particle size was determined by the broadening of (220) reflection at about 67° (2θ) by using the Debye–Sherrer equation after correction for instrumental broadening [20]. The Pt/C catalyst showed an average particle size of 40 ± 2 Å, whereas it was 26 ± 2 Å in the Pt–Ru catalyst.

3.2. Electrochemical analysis

The electrode–electrolyte assemblies were investigated in a single cell test station. The cell test fixture was equipped with SFFs or IFFs at both anode and cathode. After installing the M&E assembly in the fuel cell housing, internal humidification and steady-state performance were achieved by operating the fuel cell with methanol

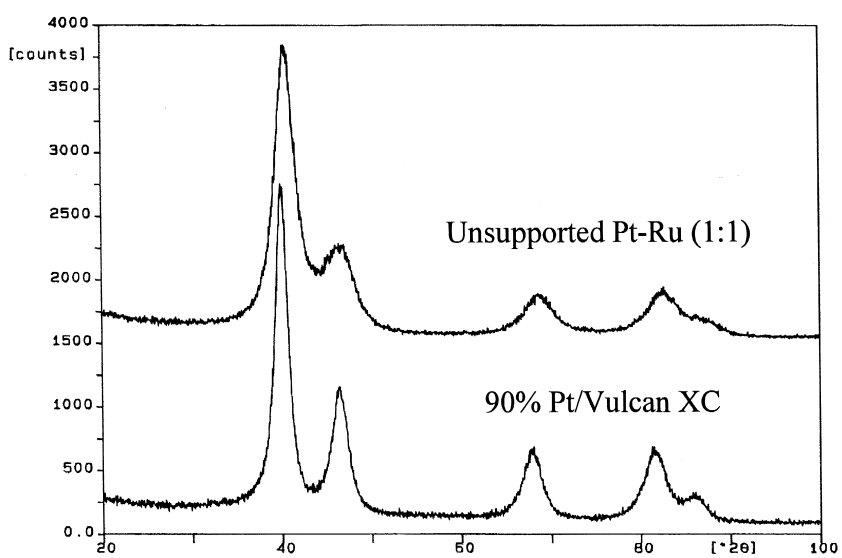

Fig. 2. XRD patterns of unsupported Pt–Ru and 90% Pt/Vulcan XC catalysts.

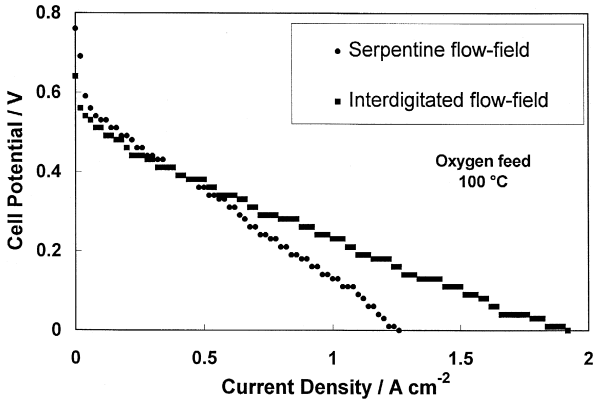

Fig. 3. Galvanostatic polarisation data for the DMFC equipped with SFFs or IFFs at 100°C in presence of 2 M methanol and oxygen feed.

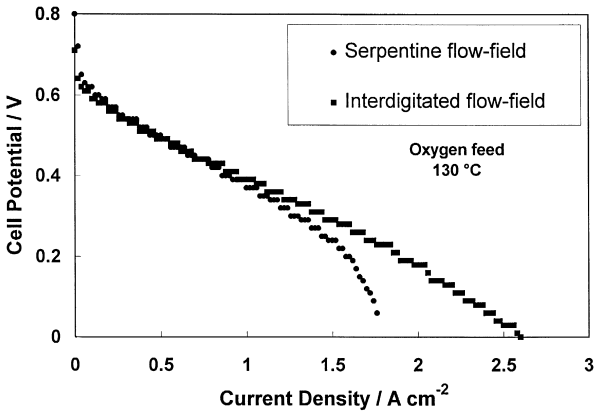

Fig. 5. Galvanostatic polarisation data for the DMFC equipped with SFFs or IFFs at 130°C in presence of 2 M methanol and oxygen feed.

(0.5 M) and oxygen (3 atm) for half day at suitable current densities (200 mA cm^{-2}). Afterwards, 1 or 2 M methanol solution was fed to the anode compartment and the electrochemical behaviour of the cell was recorded. The influence of the flow field design for the DMFC equipped with SFFs or IFFs at both anode and cathode was investigated at 100°C and 130°C. Polarisation and power density curves obtained at 100°C in the presence of oxygen feed and 2 M solution with SFFs or IFFs at anode and cathode are compared in Figs. 3 and 4. A higher open circuit voltage (OCV) is observed in the presence of the SFF, together with a lower voltage drop in the activation controlled region. Larger cell voltages have been recorded in the case of SFF up to 0.35 A cm^{-2} (Fig. 3). In the presence of the SFF, the driving force of methanol permeation through the catalytic layer is via a diffusion mechanism. Thus, a lower methanol flow towards the interface is expected with respect to the IFF, where a forced convection mechanism is favoured. At high current densities, the IFF determines lower voltage losses with respect to the SFF (Fig. 3). Besides, the cell resistance was slightly larger in the case of the SFF (0.12 vs. 0.08 Ω cm^2) probably due to the lower membrane humidification characteristics determined by the lower water/methanol flow at interface. The short circuit current density registered at 100°C in oxygen (Fig. 3) is significantly higher in the case of IFF (about 1.8 A cm^{-2}) against SFF (1.25 A cm^{-2}). It can be derived that the forced-convection mechanism induced by the IFF allows a faster mass-transport; this determines lower voltage losses in the diffusion controlled region, thus a higher limiting current density is accordingly expected compared to the conventional flow field (SFF) where a diffusion mechanism is prevailing. In terms of power density, it is observed that the maximum power outputs are recorded for both SFF and IFF at current densities above 500 mA cm^{-2}, i.e. in the region where ohmic drop and mass transport play a significant role (Figs. 3 and 4). Accordingly, the maximum power density recorded at 100°C in the presence of the IFF (240 mW cm^{-2}) is higher than that obtained with SFF; whereas, up to 0.4 V, the power output is slightly superior in the case of SFF (Figs. 3 and 4). The latter region is more significant for practical operation of the DMFC with suitable system efficiencies.

Polarisation and power density curves for the DMFC equipped with SFFs or IFFs at 130°C in the presence of oxygen feed are shown in Figs. 5 and 6. Operation at higher temperatures enhances methanol reaction kinetics,

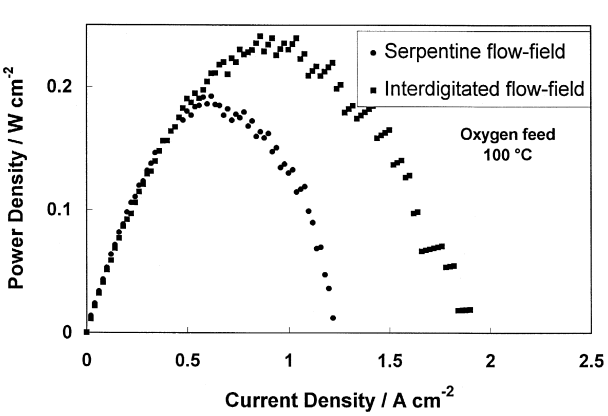

Fig. 4. Power density curves for the DMFC equipped with SFFs or IFFs at 100°C in presence of 2 M methanol and oxygen feed.

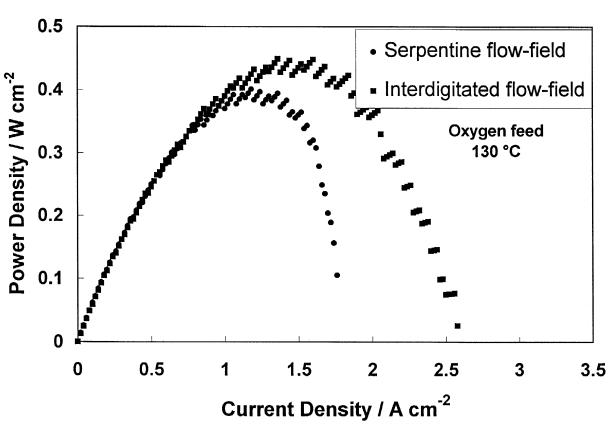

Fig. 6. Power density curves for the DMFC equipped with SFFs or IFFs at 130°C in presence of 2 M methanol and oxygen feed.

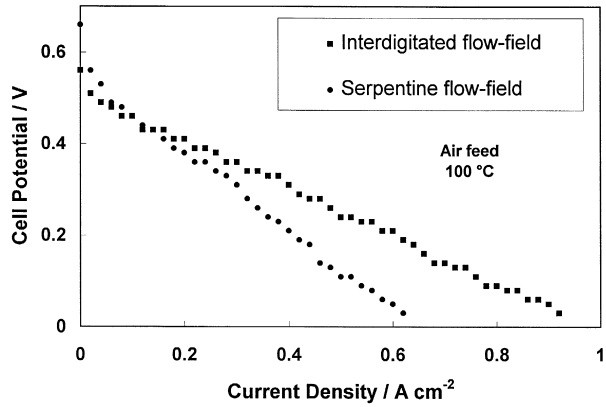

Fig. 7. Galvanostatic polarisation data for the DMFC equipped with SFFs or IFFs at 100°C in presence of 2 M methanol and air feed.

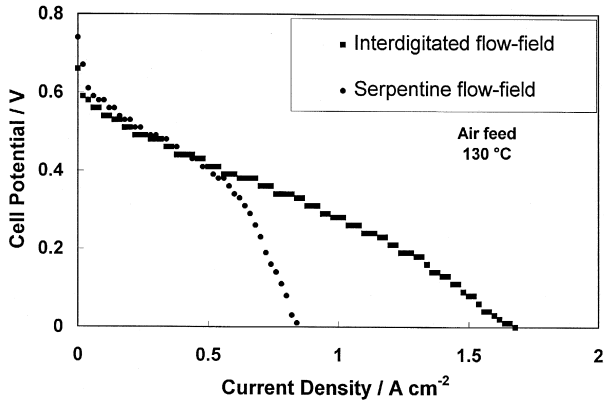

Fig. 9. Galvanostatic polarisation data for the DMFC equipped with SFFs or IFFs at 130°C in presence of 2 M methanol and air feed.

and as a consequence, higher OCVs are recorded in the presence of both flow field designs. The characteristic behaviour previously observed at 100°C for IFF and SFF is still observed at 130°C (Fig. 5). The SFF gives rise to higher OCV and slightly better performance in the activation controlled region, whereas the IFF results in significantly higher cell voltages in the mass transport controlled region. However, the voltage gap between SFF and IFF at low current densities is much less significant at 130°C with respect to 100°C and there is almost no difference in the range between 0.6 and 0.4 V (Fig. 5). This effect is likely due to the more efficient methanol consumption at electrode–electrolyte interface, which reduces the effective concentration of unreacted methanol in the proximity of the membrane. Thus, the methanol concentration gradient across the membrane is almost similar for both flow designs. Furthermore, due to the enhancement of reactant mass transport induced by the increase of temperature, the polarisation curves become significantly different only at low cell voltages (below 0.3 V). The observed short circuit current density of 2.6 A cm^{-2} with IFF indicates that optimal mass transport conditions are achieved (Fig. 5). The maximum power outputs are about 400 and 450 mW cm^{-2} for SFF and IFF DMFCs, respectively (Fig. 6). At a reference cell voltage of 0.5 V, the power density output is about 270 mW cm^{-2} in both cases (Fig. 6). These results favourably compare to those reported for DMFCs based on Nafion 112 membrane under similar operation conditions (130°C, pressurised cell, 2 mg Pt cm^{-2}) but employing unsupported Pt–RuO_x catalyst at the anode [1,7]. Probably, the absence of RuO_2 crystallographic phase in the present Pt–Ru alloy catalyst (see Fig. 2) produces and increase of labile-bonded oxygen species on the surface with respect to the strongly bonded oxygen atoms. According to the bifunctional theory [21], labile-bonded oxygen species promote the oxidation of chemisorbed methanol derived-species through a surface reaction.

The DMFC polarisation behaviour in the presence of air as oxidant is shown in Figs. 7–10. Compared to oxygen-fed DMFC, lower OCVs and short circuit current densities, as well as inferior performance is observed at both temperatures (100 and 130°C) for the air-fed DMFC (Figs. 7–10). The effect of cathode poisoning by methanol is quite significant at 100°C in presence of air (Fig. 7). The low oxygen partial pressure does not counteract efficiently the negative effects of methanol chemisorption on the cathode surface. The maximum power output in the presence of air

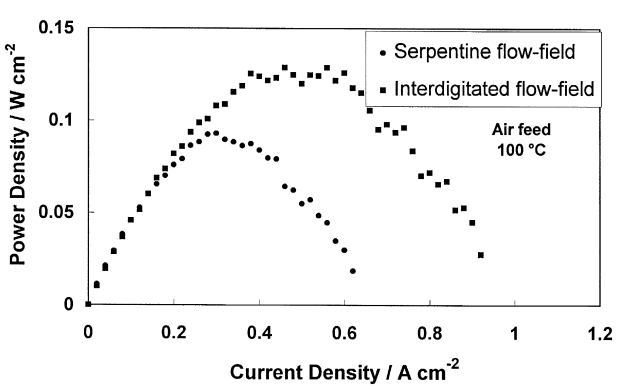

Fig. 8. Power density curves for the DMFC equipped with SFFs or IFFs at 100°C in presence of 2 M methanol and air feed.

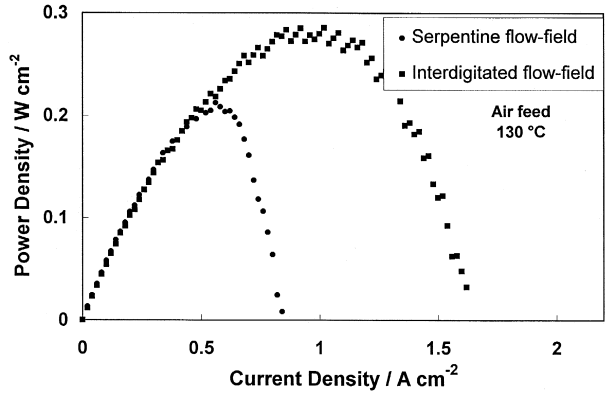

Fig. 10. Power density curves for the DMFC equipped with SFFs or IFFs at 130°C in presence of 2 M methanol and air feed.

at 100°C is approaching 140 mW cm^{-2} (Fig. 8). The higher methanol oxidation rates achieved at 130°C, determine a lower activation control (Fig. 9). As previously observed for the oxygen-fed DMFC, the polarisation behaviour at low current densities is almost similar for both flow field geometries, whereas, a significantly better performance is achieved in the high current density region with the IFF allowing to achieve a short circuit current density of 1.6 A cm^{-2} and a maximum power output of 290 mW cm^{-2} (Fig. 10). All polarisation curves, previously shown, have been obtained with 2 M methanol anode feed. As reported in a previous paper [18], the choice of this concentration derives from the compromise between the various factors governing fuel cell performance, i.e., methanol electro-oxidation kinetics, mass transport and cross-over through the membrane. In terms of reaction kinetics, a high water/methanol ratio favours the water displacement reaction, whereas, an increase of methanol concentration produces a larger methanol chemisorption on the catalyst surface. According to the bifunctional theory [21], the maximum oxidation rate is achieved when the coverage of OH species on Ru sites and methanol-derived species on Pt sites are comparable and the adsorbed species are well mixed on an atomic scale. An increase of methanol concentration reduces diffusional limitations, but leads to an increase of methanol cross-over through the electrolyte. Yet, even if a 2-M methanol concentration is a good compromise for the SFF-DMFC, the negative effects of methanol cross-over registered in presence of an air-fed fuel cell equipped with IFFs, have prompted us to investigate the cell behaviour in presence of lower methanol concentrations. The polarisation behaviour and power density output of an air-fed IFF-DMFC in presence of 1 and 2 M methanol feed are shown in Figs. 11 and 12. The DMFC fed with 1 M methanol concentration shows higher cell performances up to 0.8 A cm^{-2} (Fig. 11), indicating that the methanol cross-over plays a significant role in decreasing cell performance under air operation. Mass-transport characteristics are enhanced by 2 M methanol concentration as expected (Fig. 11). An almost similar maximum power output of 290 mW cm^{-2} is

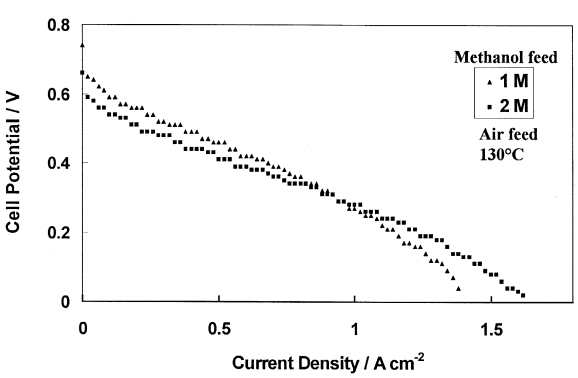

Fig. 11. Comparison of the polarisation data for the air-feed IFF-DMFC in presence of 1 or 2 M methanol solution.

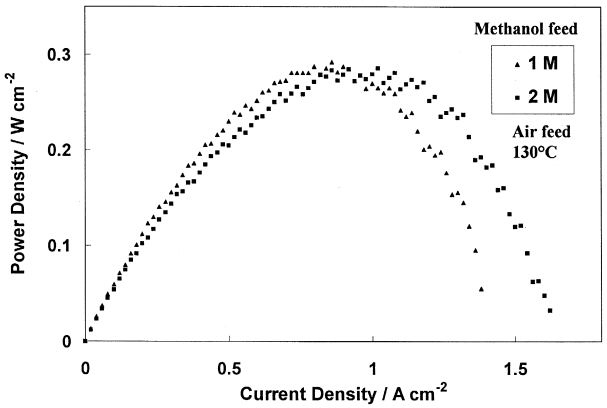

Fig. 12. Power density curves for the air-feed IFF-DMFC in presence of 1 or 2 M methanol solution.

observed at both concentrations (Fig. 12), but higher voltage efficiency is obtained with 1 M methanol feed at low and intermediate current densities. At a cell voltage of 0.5 V, a 200 mW cm^{-2} output power density is observed in presence of 1 M methanol concentration (Fig. 12). In terms of mass transport, the short circuit current density achieved with 1 M methanol feed in presence of IFF is still much higher than that observed in presence of 2 M and SFF (compare Figs. 9 and 11). Thus, operation of the DMFC with IFF and lower methanol concentration at anode allows one to achieve higher voltage efficiencies, still maintaining the suitable mass-transport properties, which are typical of the forced convection mechanism.

3.3. Methanol cross-over

Comparing the polarisation behaviour of the IFF and SFF-DMFC, we have derived that a larger methanol cross-over occurs when the cell is equipped with the IFFs. To experimentally validate such hypothesis, the cathode outlet stream was chromatographically analysed by sampling with a syringe a dried gas sample in order to determine the rate of CO_2 formation at cathode during fuel cell operation under a constant current density of 500 mA cm^{-2} both in presence of SFF and IFF. In a similar experiment, the exhaust liquid of the cathode was collected in a condenser and analysed in order to detect unreacted methanol. It was observed that in presence of both IFFs and SFFs, the amount of unreacted methanol was only a small amount (5–10%) of the overall methanol cross-over, since most of the methanol permeated to the cathode compartment was oxidised to CO_2 at the Pt surface. The amount of methanol cross-over at 130°C in presence of 2 M methanol feed was 11.5×10^{-6} and 5.6×10^{-6} mol min^{-1} cm^{-2} for the DMFC equipped with IFF and SFF, respectively. In the presence of 0.5 M methanol feed, the IFF-DMFC showed a methanol cross-over of 4×10^{-6} mol min^{-1} cm^{-2}. The methanol cross-over for the 1 M IFF-DMFC is almost comparable to the 2 M SFF DMFC.

The overall efficiency of a methanol fuel cell is determined by both voltage efficiency and fuel efficiency. The fuel efficiency is mainly influenced by the methanol cross-over through the membrane. If we express the methanol cross-over in terms of current density that is practically lost in the parasitic reaction occurring at the cathode, $I_{\text{cross-over}}$, the fuel efficiency is determined by :

$$\eta_{\text{fuel}} = \frac{I_{\text{cell}}}{I_{\text{cross-over}} + I_{\text{cell}}}$$

where I_{cell} is the measured current density. Accordingly, at a practical current density of 500 mA cm^{-2} and in presence of 2 M methanol feed, the fuel efficiency is about 82% in the case of IFF, whereas it is 90% in the case of SFF at 130°C. When the IFF is combined with 1 M methanol feed, a fuel efficiency of almost 90% is obtained.

Methanol cross-over through a perfluorosulfonic membrane is governed by the electrolyte characteristics and by various factors such as temperature and pressure conditions, concentration gradient, transport of reactants to the electrode–electrolyte interface, current density, etc.. The current density determines both the amount of methanol, which crosses the membrane due to the electro-osmotic drag and the rate of methanol consumption at the interface. Although electro-osmotic drag increases with the increase of current density, previous studies have shown that the amount of methanol cross-over decreases with the increase of current density, since it is efficiently consumed at the interface [22]. Such evidence would also imply that the concentration of methanol at the interface is larger in the case of IFF, because of the higher mass transfer coefficient. This mechanism determines the higher methanol cross-over rates in presence of the IFF.

3.4. Membrane humidification

The action of the IFF does not only concern an enhancement of mass-transport inside the cell but also induces a better humidification of the membrane with consequent reduction of ohmic constraints. In fact, it can be observed that the slope of the polarisation curves at intermediate current densities, where the electrochemical reaction is under ohmic control, is larger in the presence of the SFF at both temperatures. This reflects a higher ionic resistance due to a limited water supply to the membrane. The cell resistance values observed in the presence of SFF are 0.12 and 0.08 Ω cm^2 at 100°C and 130°C, respectively, whereas in the presence of the IFF these are 0.08 and 0.06 Ω cm^2. The poisoning effect determined by methanol cross-over in the presence of the IFF is thus, entirely recovered, at high current densities, by the positive effects of better membrane humidification and a more effective reactant supply.

4. Conclusions

The IFFs significantly enhance mass-transport inside a DMFC allowing to achieve higher maximum power outputs compared to the classical serpentine geometry. Two aspects related to the use of IFFs in DMFC devices have been evidenced, i.e., a larger methanol cross-over through the polymer membrane and a better membrane humidification at high temperatures. Both aspects are strictly related with the forced-convection mechanism for the reactant flows inside the cell. The larger methanol permeation through the electrolyte determines both lower voltage and fuel efficiencies in the activation controlled region with respect to the SFF. Thus, appropriate methanol concentrations (1 M) must be selected for the anode feed in order to combine suitable electrochemical efficiency with efficient mass transport and power outputs. The enhanced water transport at the electrode–electrolyte interface maintains an appropriate membrane hydration and, thus, a low ionic resistance is observed even when the methanol fuel cell is operated at high temperatures.

Acknowledgements

The authors are grateful to Dr. K. M. El-Khatib (National Research Center, Dokki, Giza, Egypt) for the co-operation and helpful discussions.

References

[1] X. Ren, M.S. Wilson, S. Gottesfeld, J. Electrochem. Soc. 143 (1996) L12.
[2] S.R. Narayanan, W. Chun, T.I. Valdez, B. Jeffries-Nakamura, H. Frank, S. Surampudi, G. Halpert, J. Kosek, C. Cropley, A.B. LaConti, M. Smart, Q. Wang, G. Surya Prakash, G.A. Olah, Program and Abstracts, Fuel Cell Seminar (1996) 525–528.
[3] M. Baldauf, W. Preidel, J. Power Sources 84 (1999) 161.
[4] A.K. Shukla, P.A. Christensen, A. Hamnett, M.P. Hogarth, J. Power Sources 55 (1995) 87.
[5] K. Scott, W.M. Taama, P. Argyropoulos, K. Sundmacher, J. Power Sources 83 (1999) 204.
[6] A.S. Aricò, P. Creti, P.L. Antonucci, V. Antonucci, Electrochem. Solid-State Lett. 1 (1998) 4.
[7] A.S. Aricò, A.K. Shukla, K.M. el-Khatib, P. Creti, V. Antonucci, J. Appl. Electrochem. 29 (1999) 671.
[8] A. Hamnett, Philos. Trans. R. Soc. London, Ser. A 354 (1996) 1653.
[9] M.P. Hogarth, G.A. Hards, Platinum Met. Rev. 40 (1996) 150.
[10] C. Lamy, J-M. Léger, in: O. Savadogo, P.R. Roberge (Eds.), Proc. Second International Symp. On New Materials for Fuel Cells and Modern Battery Systems, Montrèal, Canada,1997, pp. 477–487.
[11] A. Küver, W. Vielstich, J. Power Sources 74 (1998) 211.
[12] T.V. Nguyen, J. Electrochem. Soc. 143 (1996) L103.
[13] M.S. Wilson, T.E. Sringer, J.R. Davey, S. Gottesfeld, in: S. Gottesfeld, G. Halpert, A. Langrebe (Eds.), Proton Conducting Membrane Fuel Cells I, PV 95-23, The Electrochemical Society Proceedings Series, Pennington, NJ, 1995, p. 115.

[14] D.L. Wood, J.S. Yi, T.V. Nguyen, Electrochim. Acta 43 (1998) 3795.
[15] L. Liu, C. Pu, R. Viswanathan, Q. Fan, R. Liu, E.S. Smotkin, Electrochim. Acta 43 (1998) 3657.
[16] J.S. Yi, T.V. Nguyen, J. Electrochem. Soc. 146 (1999) 38.
[17] H.G. Petrow, R.J. Allen, U.S. Pat. 3, 992, 331 (1976).
[18] A.S. Aricò, P. Creti, P.L. Antonucci, J. Cho, H. Kim, V. Antonucci, Electrochim. Acta 43 (1998) 3719.
[19] H.A. Gasteiger, P.N. Ross Jr, E. Cairns, J. Surf. Sci. 67 (1993) 293.
[20] A.S. Aricò, P. Creti, H. Kim, R. Mantegna, N. Giordano, V. Antonucci, J. Electrochem. Soc. 143 (1996) 3950.
[21] M. Watanabe, S. Motoo, J. Electroanal. Chem. 60 (1975) 275.
[22] S. Cleghorn, X. Ren, S. Thomas, S. Gottesfeld, Book of Extended Abstracts, 1997 ISE-ECS Joint Symposium, Paris, Sept. 1997, Abstract no. 182, pp. 218–219